

Pulverized rocks in the Mojave section of the San Andreas Fault Zone

Ory Dor ^{a,*}, Yehuda Ben-Zion ^a, Thomas K. Rockwell ^b, Jim Brune ^c

^a Department of Earth Sciences, University of Southern California, Los Angeles, CA 90089-0740, USA

^b Department of Geological Sciences, San Diego State University, San Diego, CA 92182-1020, USA

^c Nevada Seismological Laboratory, University of Nevada, Reno, NV 89557, USA

Received 29 May 2005; received in revised form 21 March 2006; accepted 23 March 2006

Available online 5 May 2006

Editor: R.D. van der Hilst

Abstract

We present mapping of pulverized fault zone rocks along a 140 km long section of the San Andreas Fault in the Mojave Desert. The results show that almost every outcrop of crystalline rock within about 100 m wide belt along this fault section is pulverized and lacks significant shear. We find structural similarities between the San Andreas Fault zone and exhumed faults of the San Andreas system, although pulverized rocks are not common in all of them. About 70% of the pulverized fault zone rocks appear on the northeast side of the principal slip zone of the San Andreas Fault, possibly reflecting an asymmetric structure of the damage zone. Detailed mapping at selected sites, as well as previous mapping of rock damage at smaller scales, are consistent with the large-scale asymmetric pattern of the pulverized rocks. A possible pulverization of sedimentary rocks, inferences from regional uplift indicators, and theoretical considerations imply that pulverization along this portion of the fault occurred in the top few km of the crust. The width of the pulverized fault zone rocks and inferred depth extent of pulverization are similar to the dimensions of imaged low velocity fault zone layers that act as waveguides for seismic trapped waves. The side of the fault that appears to sustain more damage is the block with faster seismic velocities at seismogenic depth. This correlation and the inferred shallow depth for pulverization are compatible with predictions for wrinkle-like ruptures along a material interface, with a preferred northwest propagation direction of large earthquakes on the Mojave section of the fault.

© 2006 Elsevier B.V. All rights reserved.

Keywords: earthquake physics; geologic mapping; fault zone structure; rock damage; dynamic rupture; pulverized rocks

1. Introduction

The term Pulverized Fault Zone Rocks (PFZR) refers mainly to crystalline plutonic and metamorphic rocks that were mechanically pulverized to the micron or finer scale, while preserving most of their original fabric and crystal boundaries. Outcrops of such rocks were

observed long ago but little attempt was made to characterize them systematically until Brune [1] noted the lack of significant shear parallel to the San Andreas Fault (SAF) within PFZR in several locations. Those findings were followed by the detailed study of Wilson et al. [2] in a road cut exposure of Tejon Lookout granite adjacent to the slip zone of the SAF at Tejon Pass. They mapped the local distribution and internal structure of the PFZR and analyzed its particle size distribution. The main findings from the studies associated with the Tejon

* Corresponding author. Tel.: +1 213 740 6754; fax: +1 213 740 8801.
E-mail address: dor@usc.edu (O. Dor).

Pass exposure are: 1) The PFZR form ~ 70 – 100 m wide fault zone layer in the immediate vicinity of the localized slip. 2) There are myriad small scale fractures within the PFZR with no preference for shear parallel to the SAF. 3) The PFZR layer lacks significant amounts of weathering products and is distinctly different from gneiss (in situ accumulation of disaggregated plutonic material). 4) The PFZR layer is pervasively pulverized to the sub-micron scale.

The observations from Tejon Pass confirm that the observed pulverization is the result of mechanical processes rather than a weathering product. In addition, the abundance of tension features and the extreme reduction of grain size without distortion of the rock fabric imply that the protolite of the PFZR was subjected to a strong tensional stress, apparently due to dynamic reduction of normal stress associated with slip during SAF earthquakes. Brune et al. [3] observed in laboratory experiments with foam rubber blocks that the passage of rupture is correlated with significant reduction of normal stress associated with vibrations normal to the interface and separation during slip. A summary of several mechanisms that can produce dynamic reduction of normal stress during earthquake ruptures is given by Ben-Zion [4]. These include acoustic fluidization [5], collisions of rough surfaces [6] and a variety of fluid effects (e.g., [7–9]).

Another possible mechanism for strong dynamic reduction of normal stress across large faults, with testable predictions on the structure of those faults, is rupture along a material interface that separates different solids (e.g., [10–13,4]). Numerical simulations show that mode II ruptures on a bimaterial interface tend to evolve for ranges of conditions with propagation distance to wrinkle-like ruptures with several characteristic features (e.g., [14–18]). These include: (1) a preferred or more vigorous direction of rupture propagation that is the same as the direction of slip in the slower velocity (more compliant) solid, (2) strong dynamic reduction of normal stress at the tip propagating in the preferred direction, (3) strongly asymmetric motion across the fault, and (4) tendency of the rupture-tip region with significant slip-velocity to become narrower and higher with propagation distance. Property (1) has implications for the symmetry properties of the damage pattern generated by many earthquakes on the fault. Properties (2–4) can produce tensile dynamic stress field leading in some conditions to “opening modes” of rupture. In some ranges of parameters these characteristics exist only in a weak form (e.g., [19]). See related discussion in Ref. [20].

Earlier studies [21,22] suggested that significant off-fault damage is produced only in the vicinity of fault

jogs (and other geometrical complexities). The consistency of pulverization along the entire relatively straight Mojave section of the SAF (see below) suggests that the observed pulverization is the outcome of a fundamental dynamic property of earthquake ruptures rather than a site-related effect. Theoretical and numerical studies of dynamic ruptures indicate that off-fault damage occurs primarily in the tensional quadrants of the radiated fields [23–28]. If earthquakes on a given fault section propagate predominately as bilateral ruptures, or as unilateral ruptures without a preferred propagation direction, the cumulative pattern of rock damage generated by many events will be approximately symmetric across the fault. However, if earthquakes on a given fault section have a preferred propagation direction, the cumulative damage pattern will be asymmetric, with more damage in the tensional quadrant associated with the preferred propagation direction. Ben-Zion and Shi [27] simulated dynamic ruptures along a bimaterial interface in a model that includes spontaneous generation of damage in the bulk. The results show that in such cases, damage is generated primarily on the stiffer side of the fault, which is in the tensional quadrant of the radiated seismic field for the preferred propagation direction. Damage generation is enhanced by the dynamic reduction of normal stress at the propagating tip, and the zone of intense damage has an approximately constant width that is related to the rupture pulse width. The simulations of Ben-Zion and Shi [27] suggest further that significant generation of rock damage, under realistic conditions of velocity contrast and material properties, is limited to the top few km of the crust. See also Ref. [28]. Thus, the generated damage does not affect significantly the velocity structure at depth that controls the rupture dynamics. The above results provide clear predictions that can be tested by geologic observations of rock damage across large strike slip faults.

Recent observational studies provided information on symmetry properties of off-fault damage. Dor et al. [29] performed detailed geological mapping of rock damage over fault core scales of ~ 0.01 – 1 m and fault zone scales of ~ 1 – 10 's of m in the structures of the SAF, San Jacinto Fault and the Punchbowl Fault in southern California. They observed consistent asymmetry in the distribution of gouge and fault zone damage across the principal slip zones of those faults. For cases where the velocity structure of the fault is known they showed that considerably more damage appears on the crustal blocks that have faster seismic velocities at depth [30–33]. High resolution imaging of the local velocity structure of the San Jacinto fault zone based on seismic

trapped waves [34] indicates the existence of a 100 m wide damaged fault zone rock in the top 3–5 km of the crust, with a similar sense of asymmetry as in the geological mapping of Dor et al. [29]. Inversion of fault zone head and direct *P* waves in the Bear valley section of the SAF also suggest the existence of a shallow damage zone that is shifted toward the faster velocity block [35].

In this work we present geologic mapping of PFZR along the Mojave section of the SAF, with a focus on the overall large-scale properties of the PFZR. Complementing the mapping of Dor et al. [29] over smaller scales of observations, we provide mapping results over a damage zone scale of ~10–100's of m. Our observations show that PFZR are common along the SAF in the Mojave and probably occupy a ~100 m wide tabular sub-vertical zone parallel to the fault. In addition, we find that the distribution of the exposed PFZR is not symmetric with respect to the principal slip zone, but is shifted on the average to the northeast side of the fault. Based on several observational arguments (mainly field relations between different rock units and the apparent damage found in sedimentary rocks), we infer that the observed pulverization occurred in the top few km of the crust. The large-scale properties of the mapped body of PFZR appear to be similar to those associated with fault zone seismic waveguide structures. The observations are compatible with predictions for rupture along a material interface.

2. Observations

2.1. Approach

Our study area spans the Mojave section of the SAF between approximately Tejon pass and Cajon pass (Fig. 1). This section of the fault was chosen to extend the smaller scale observations of Dor et al. [29], to provide a regional

context for the detailed studies of Wilson et al. [2] at Tejon pass, and for the following additional reasons. (1) The geometry of the fault along the mapped stretch is relatively simple; the fault section is near-vertical, relatively straight, and the big bends of the SAF are outside the mapping area. (2) Large portions of this fault section lie within an arid climate area and the fault zone rocks crop out in many places. Further, some fault sections are situated within or at the margins of locally uplifted terrains which promote exposure. (3) Detailed geologic mapping of the fault between Quail Lake and Big Pine is available by Barrows et al. [36]. Thus this is an excellent working platform that includes 1:12,000 geologic strip maps and 1:12,000 aerial photos, both with delineated traces of the small and large faults of the SAF system. These resources assisted us in locating exposures of crystalline rocks in the vicinity of the fault. As part of their mapping, Barrows et al. [36] described some of the granitic rock bodies near the SAF as “powdery, crumbly, microbreccia locally well developed but shearing not everywhere intensive enough to obscure original igneous textures” and “shattered and crushed to white powder”. Yet, they did not map the extent of pulverization systematically. The section of the SAF between Big Pine and Cajon Pass is covered by a map [37] of recently active breaks at a scale of 1:24,000.

We concentrate primarily on mapping pulverized and damaged crystalline plutonic and metamorphic rocks (referred to below as ‘crystalline’). The number of exposures associated with crystalline rocks is sufficiently large to indicate a significant pattern, yet can be covered by a reasonable mapping effort. In addition, we discuss results associated with a few exposures of fault zone rocks of sedimentary origin. The crystalline rocks can potentially express conditions and processes from various crustal depths. This is in contrast to Plio-Quaternary sandstones and other deposits along the SAF that were never deeply buried. Mapping and damage characterization of these types of rocks provide

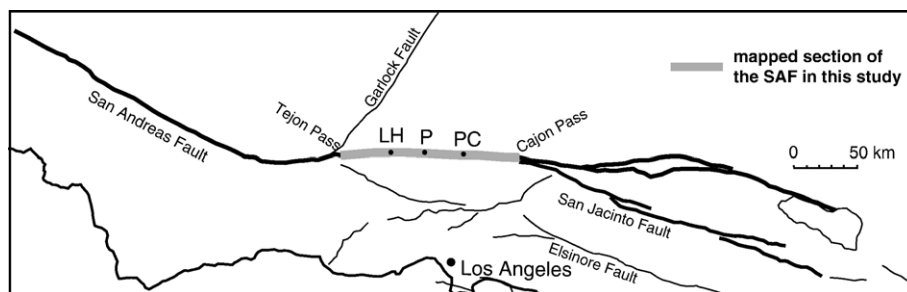


Fig. 1. The south central San Andreas Fault (SAF) system with its major strands. Mapping of pulverized fault zone rocks in this work covers a 140 km stretch of the SAF in the Mojave, indicated with a thick grey line. Geographic reference points are indicated: LH: Lake Hughes; P: Palmdale; PC: Pallett Creek.

important constraints for the depth generation of pulverization and associated dynamic fields.

PFZR are distinct geologic features with unique appearance, texture and morphology that enable relatively easy identification in the field. We use the term PFZR for rocks with texture similar to that of the pulverized granite in Tejon Pass [2]. In general, outcrops of PFZR, including the one in Tejon Pass, share similar morphology, frequently typified by bad-land topography and high drainage density. Although the ultimate quantification and classification of pulverization (e.g. chemistry and mineralogy, particle size distribution, crack orientations) require lab work, PFZR can be classified in situ for field mapping purposes according to macroscopic properties that designate a relative class of damage. We label a given volume of rock as “pulverized” if all the crystals in a hand sample, including the quartz crystals, yield a powdery rock–flour texture when pressed by hand, and when the entire rock volume shows such a texture pervasively. Rocks

are identified as “selectively pulverized” when only some of the crystals yield powdery texture or only certain rock domains within the exposure are pulverized. Both “pulverized” and “selectively pulverized” rocks show very little or no shear and their original fabrics are preserved including crystal shapes, crystal boundaries, and magmatic fabrics. PFZR may still contain small faults that are insignificant as displacement carriers in the parent structure. Both types of rocks may show fabric similar to that of the original undamaged rock, but they can be penetrated and pressed to powder by hand and hence considered here as PFZR. We further differentiate the classes of pulverization in Section 2.3 that describes higher resolution mesoscale mapping.

Figs. 2 and 3 present mapping results of all the accessible exposures of crystalline plutonic rocks within ~400 m wide strip centered on the main trace of the SAF in the Mojave between Quail Lake and Cajon Pass. The map of Fig. 2 includes only rocks that are actually exposed with minimum interpolation of the rock and damage type

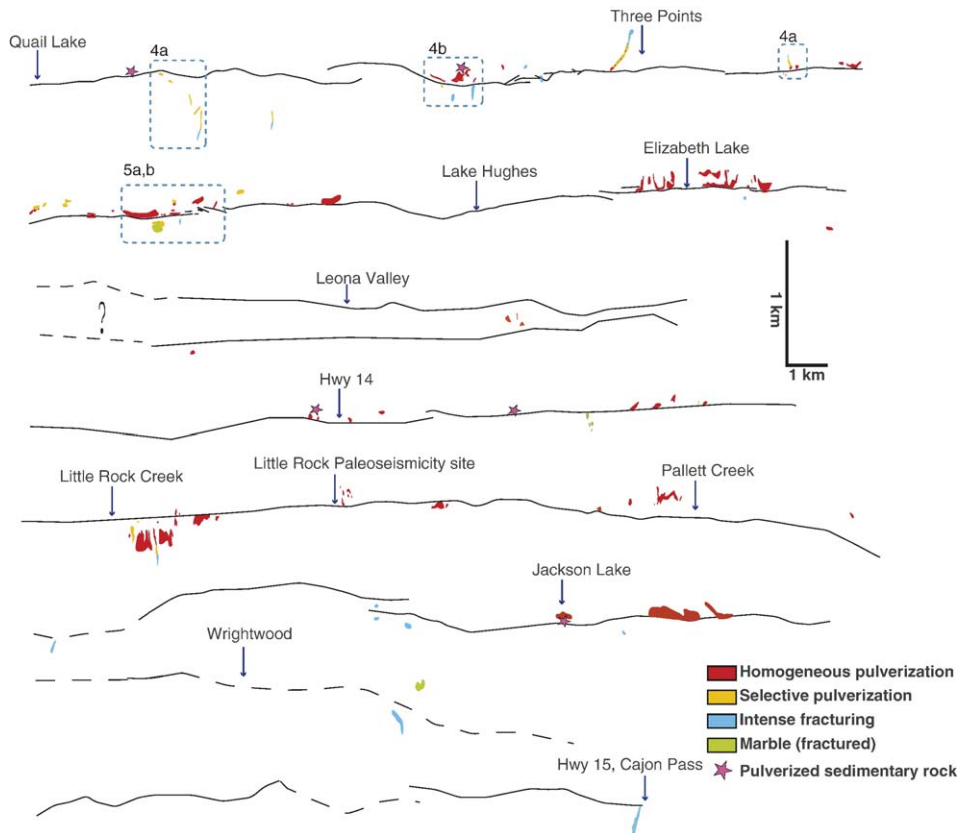


Fig. 2. Map of crystalline plutonic rocks in the damage zone of the SAF, classified according to their damage pattern (color scale). Also shown are exposures of damaged to pulverized sedimentary rocks (purple stars). The map covers a 140 km long section of the fault between Quail Lake and Cajon Pass. The fault-normal dimension was enlarged to be three times the fault parallel dimension, causing an artificial distortion of the fault trace. The pulverized fault zone rocks (red and orange spots) were found mainly on the northeast side of the fault. Blue dashed frames show sections for which mesoscale mapping are presented in Figs. 4 and 5.

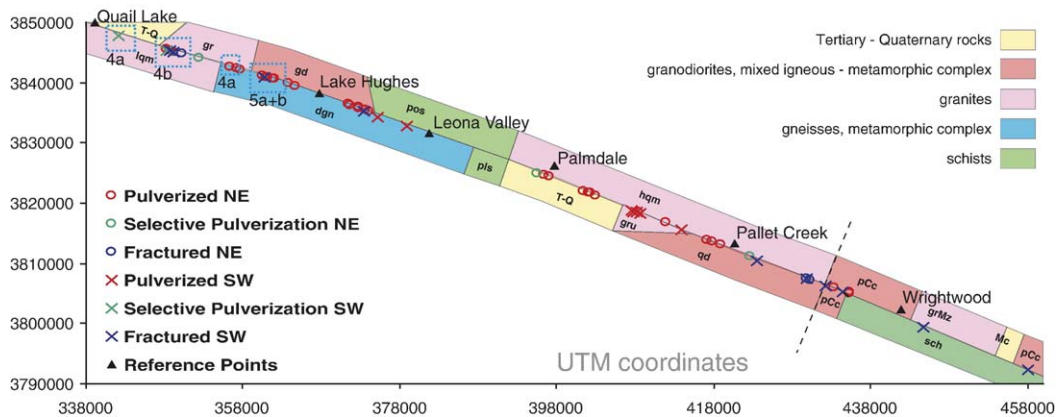


Fig. 3. A large-scale distribution pattern of crystalline rocks and their damage pattern between Tejon Pass and Cajon Pass. Each data point represents an outcrop. The pulverized fault zone rocks (red and green marks) are abundant along the fault, especially on its northeast side (circles). Annotated frames mark locations of the detailed mapping of Figs. 4 and 5. The colored strips generalize the distribution pattern of classes of crystalline rocks that crop out, often sporadically, within a few km from the fault (the width of the strips is not to scale). This distribution follows the mapping of Barrows et al. [36] between Quail Lake and the dashed line south of Pallett Creek, and the mapping of Jennings et al. [38] from there to Cajon Pass. The Alphabetic codes within the strips correspond to further classification of the rock types in the original geological maps.

between exposures (e.g., below stretches of alluvium). We minimized interpolation because the pattern of pulverization, which is the essence of our mapping, can change rapidly over a short distance. If PFZR are exposed with no lateral width (e.g., in vertical road cuts) they are given a minimum width of about 10 m. Fig. 3 simplifies the pattern of Fig. 2 by showing the location of the mapped classified outcrops. The colored strips show the dominant types of crystalline rocks that crop out up to a few km from the fault. The width of the strips is not to scale and was chosen for graphical reasons.

The mapped outcrops of PFZR were digitized in a GIS format on a spatially referenced 1:24,000 map on the basis of the field mapping. The digitized map enables a more quantitative description of the distribution of PFZR (e.g., evaluation of symmetry properties) and it provides an accurate spatial reference for later studies. The GIS-based map is included as an electronic supplementary material of the paper. Errors in the shape, location and calculated area of outcrops of the PFZR in the GIS-based map may result from two possible sources. (1) Errors during mapping in the field while projecting the boundaries of outcrops on the paper map. This applies also to the map of Fig. 2. (2) Errors during digitization of the outcrops on the raster background spatially referenced map based on the pattern in the paper map. These sources of error are assumed to have negligible influence on the evaluation of the above parameters due to high resolution of the paper and digital maps (1:12,000 and 1:24,000).

This study aims at presenting observed macroscopic properties of PFZR that are consistent at many sites along the Mojave section of the SAF. The results

provide a spatial framework for future detailed microstructural and laboratory characterization of the PFZR. The main features of our observations are described in the following sections.

2.2. Spatial distribution of PFZR in the San Andreas damage zone, Mojave

2.2.1. Distribution along the fault

In the map of Fig. 2, PFZR are shown with red and orange colors while less damaged rocks are shown in blue. The results indicate that the vast majority of crystalline rocks cropping out within 50 to 200 m of the SAF are pulverized to some degree. This is confirmed by GIS analysis, showing that 93% of the total area of mapped outcrops is covered by pulverized or selectively pulverized rocks. Outcrops of crystalline rocks outside this zone show no pulverization, and the overall damage decreases rapidly to the background level of the country rock if no geometrical complexities exist. The observations of Figs. 2 and 3 establish the PFZR as a general structural component of the San Andreas Fault zone in the Mojave. The PFZR appear to occupy ~100 m wide sub-vertical tabular zone parallel to the fault. They represent a systematic damage product, which is generated most likely by earthquakes and hence may serve as a diagnostic of the rupture process.

2.2.2. Distribution across the fault and symmetry properties

Figs. 2 and 3 show that along the 140 km mapped stretch of the SAF in the Mojave, outcrops of PFZR are

Table 1
Cumulative area of outcrops with different damage levels SW and NE of the fault

Damage level	Cumulative area SW (m ²)	Cumulative area NE (m ²)
1 (pervasive pulverization)	126,271	330,666
2 (selective pulverization)	27,566	25,543
3 (intense fracturing)	34,683	6409

The few outcrops that appear between two fault strands are not included.

more abundant on the northeast side of the fault. A GIS-based spatial analysis of the map indicates that 70% of the total area of all outcrops of PFZR (pulverized and selectively pulverized) is located on the northeast side of the slipping zone. The detailed distribution pattern is presented in Table 1, showing the cumulative area of each outcrop class in each side of the fault. This regional distribution pattern may reflect, at least partially, the current distribution of available exposures (66% of the total area of mapped outcrops is in the northeast side of the fault), but the outcrops are distributed unevenly with respect to the fault despite lateral variability in the contrast in surface lithology across the fault, vegetation cover, slope direction and other factors. Small and isolated outcrops of PFZR on the southwest side of the

fault appear near Quail Lake and east of Elizabeth Lake. In addition, there is a fairly large concentration of PFZR on the southwest side of the fault between Cheseboro road and E 106th St. near Little Rock Creek. Some outcrops in the Leona Valley area and west of Big Rock Creek appear between two fault strands. All the other outcrops of PFZR appear to be northeast of the fault. In contrast, outcrops of fractured rather than pulverized rocks (blue spots in Fig. 2) immediately near the fault are more abundant on the southwest side, especially between Pallett Creek and Cajon Pass.

An asymmetric pulverization across the fault may be the result of various reasons not related to rupture behavior (see related discussions below), and the apparent asymmetric pattern in Figs. 2 and 3 and Table 1 may be affected by asymmetric outcrop availability. Yet, a likely explanation for the results is that the observed distribution reflects an average shift of the PFZR layer to the northeast side of the principal slip zone. Moreover, an asymmetric damage generation is expected to produce asymmetric outcrops availability because pulverization and damage promote erodibility and exposure. A second-order measure of asymmetry is the fraction of area covered by PFZR out of the total mapped area in each side of the fault. Based on the mapping results, these fractions are 98% and 82% on the northeast and southwest sides of the fault, respectively. Similar sense of asymmetry in the damage structure was

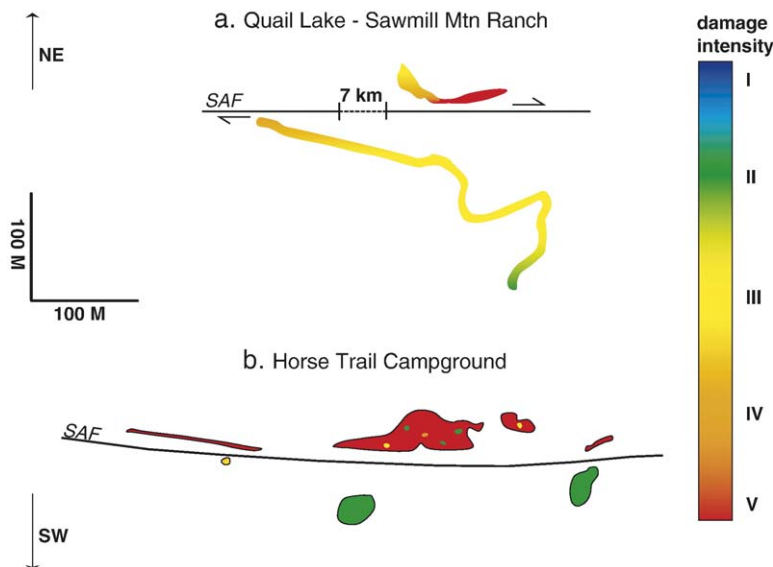


Fig. 4. A detailed distribution of damaged fault zone rocks in Quail Lake–Sawmill Mtn Ranch (a) and in Horse Trail Campground (b). The color scale corresponds to the degree of damage discussed in the text. Note the asymmetric damage pattern with more intense pulverization and wider zone of pulverized rocks on the northeast side in the two sites. The locations of these sites are shown in Figs. 2 and 3. For comparison of damage pattern between the two sides of the fault, we re-juxtaposed in (a) exposures that are currently 7 km apart, reflecting the likely geologic state ~ 200,000 years ago.

found in the smaller scale observations of Dor et al. [29] at selected sites in our study area and is compatible with our mesoscale mapping described below.

Although the mapped fault section is relatively straight and does not include major structural complexities, geometrical complexities at smaller scales may exist and affect the local faulting environment and damage pattern. The rocks surrounding the slipping zone may have been subjected to changes in the local faulting conditions during their history. However, rock bodies on the opposite sides of the fault should have had an equal chance to be exposed to local geometrical complexities. Despite these (and other) complexities, the distribution of PFZR is apparently asymmetric across the fault, while maintaining overall consistent width and pulverization gradient with respect to the slipping zone. These observations suggest that the regional body of PFZR was created by many earthquake ruptures over a time scale much longer than that associated with effects of local transient complexities. These different time scales allow the asymmetry and other large-scale systematic features to exist despite the overprint of local conditions.

We exclude marble (green spots in Fig. 2) from the discussion about symmetry properties because its damage

pattern has not yet been properly characterized. In general, marble rock bodies along the fault are only macroscopically fractured and not pulverized, but preliminary microscale observations in thin sections show that they have very high dislocation density and twinning [39] that can be possibly attributed to brittle faulting (e.g. [40]).

2.3. Classes of pulverization and fault zone scale mapping results

In several locations along the fault, we were able to map the damage pattern in the mesoscale and study the width and gradient of damage with respect to the principal slip zone. Mapping results from three of those locations are presented in Figs. 4 and 5. For the fault zone scale mapping, we chose locations in which PFZR have good exposures from the principal slip zone and outward. We found such locations only in the northwest portion of our mapping area (see locations in Figs. 2 and 3). For the purpose of this mapping, we differentiated the damage intensity into five classes. As with the regional mapping, the following definitions of damage intensity are based on in situ macroscopic distinct properties. Although the damage gradient is continuous

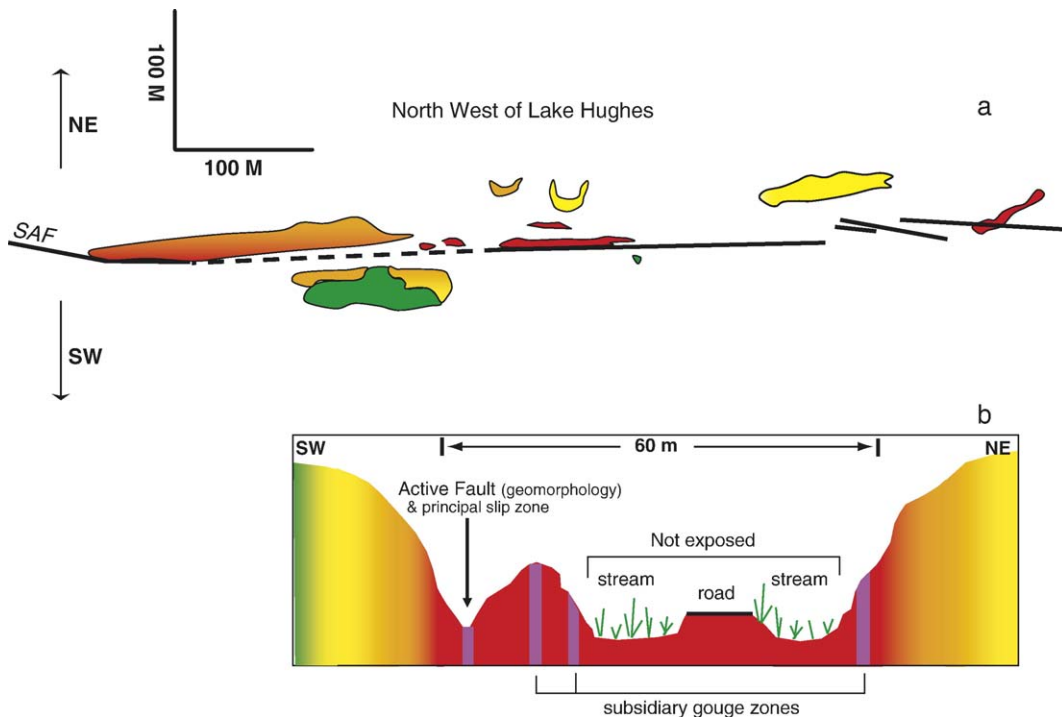


Fig. 5. (a) A detailed distribution of damaged fault zone rocks in a site northwest of Lake Hughes (see location in Figs. 2 and 3). The colors correspond to the scale in Fig. 4. (b) A schematic composite cross-section of the damage zone obtained by combining features from (a) into a vertical plane perpendicular to the fault. The principal slip zone is on the southwest side of a ~60 m wide layer of intensely pulverized rocks. Additional strike slip activity is apparent by subsidiary gouge zones northeast of the principal slip zone. A 'fault zone valley' correlates with the zone of intense damage.

without discrete transitions, we use these classes to approximate the spatial variations of damage intensity.

The classes of damage, starting from the lowest are as follows: (I) weak fracturing — macroscopic large fractures in density that exceeds the background level of damage in the country rock. (II) Fragmentation — fractures are in the cm scale and the rock is fragmented, resulting in the creation of rugged surfaces. Some of the fragments can be easily crushed by hand into smaller, visible pieces. (III) Intense fracturing — fractures are in the grain size scale. Although similar in texture to *grus*, its mechanical origin is attested by its structural context and location in the deformation gradient. It is typically characterized by rough, rounded surfaces. (IV) Weak/selective pulverization — some of the crystals survive and remain intact, some break along sub-crystal fractures, and some yield powdery texture due to microscopic fractures. The typical appearance in the field often can be similar to that of the next (highest) damage class. (V) Pervasive pulverization — all crystals yield a powdery texture when crushed by hand. Associated geomorphic landforms tend towards smooth, rounded outcrops or bad-land topography with extremely high drainage density, which is typical of very weak, easily eroded impermeable rock. Damage classes IV and V correspond to “pulverized” (red) and “selectively pulverized” (orange) in the map of Fig. 2, respectively. Damage classes I–III further differentiate the “intense fracturing” class (blue) of Fig. 2 to allow a better description of the damage gradient into the country rock.

Overall, the degree of damage of crystalline fault zone rocks at a point appears to depend mainly on the distance from and side of the fault. In addition, the damage level depends to a currently unknown extent on rock properties such as macroscopic uniformity, isotropy and the mineral content of the rock. For instance, melanocratic rocks tend to be less pulverized compared to leucocratic rocks with corresponding locations, the opposite of what would be expected from the result of *in situ* weathering. Metamorphic rocks seem to be less susceptible to pulverization, although we do not have at present independent systematic evidence for this or indication that it affects the distribution pattern of PFZR. We find on the southwest side of the fault pervasively pulverized rocks within a large body of gneisses (e.g. near Elizabeth Lake, Fig. 3) as well as macroscopically fractured rocks within granites (e.g. near Three Points, Figs. 3 and 4). The influence of the rock type on the distribution pattern of PFZR should be studied in more detail in future works.

The mesoscale mapping results of Figs. 4 and 5 provide additional information on the symmetry properties of damaged fault zone rocks with respect to the

principal slip zone of the SAF. Our mapping shows that on the northeast side of the fault, the zone of pulverization is wider and pulverization is more intense at a given distance from the fault. This is evident in Fig. 4a, displaying two road cut exposures that are currently 7 km apart, one from the Quail Lake area (south) and the other from Sawmill Mtn Ranch area (north). The exposures were re-juxtaposed for this display, reflecting a geologic situation that corresponds to about ~200,000 years ago based on the current displacement rate of 3.5 cm/year. Similar or stronger contrast in pulverization intensity is also shown clearly in Figs. 4b and 5a for two places where crystalline rocks crop out on both sides of the fault.

Fig. 5b gives a schematic composite cross-section of the damage zone in which the mapped features of Fig. 5a were combined into a vertical plane perpendicular to the fault. The resulting ~60 m wide fault zone is composed of the currently active gouge zone, as well as several other secondary gouge zones (purple lines) embedded within intensely pulverized rock (red). Although slip on the SAF could alternate between the different gouge zones, both the strong geomorphic expression of the currently active fault strand and its coincidence with the major lithologic boundary attest that this is the locus of long-term localization of motion. As such, the currently active fault strand, which is the principal slip zone, is a suitable center of reference for evaluation of symmetry properties. The subsidiary gouge zones manifest intense damage associated with faulting that is secondary to the main slip zone.

The composite cross-section of Fig. 5b has an asymmetric structure in which most of the fault zone structural elements (i.e. secondary gouge zones) and pulverization are on the northeast side of the principal slip zone. A larger scale asymmetry appears in the geomorphic expression of the SAF, with the “fault zone valley” occupying the more damaged northeast side of the fault zone.

2.4. Pulverization of sedimentary rocks

During the course of searching for crystalline rocks along the fault, we found several exposures of sedimentary rocks that exhibit damage or pulverization that correspond to degrees III to V as described above. This is supported by preliminary observations in the microscale of particle size distribution and thin sections. Those exposures are shown in Fig. 2 as purple stars and include the following sedimentary units: Juniper Hills conglomerate in several sites, Anaverde sandstone in the Palmdale area, and Hungry Valley sandstone near Three

Points and near Quail Lake. Tentative pulverization of sedimentary rocks was observed at other sites. Those damaged sedimentary rocks were found so far mainly on the northeast side of the fault. Pulverization in sedimentary units is not as abundant as in crystalline rocks, and we found several examples of nearly-intact sedimentary rocks within the fault zone at several locations (e.g. Anaverde sandstone east of Leona Valley). In places where sedimentary and crystalline pulverized rocks are found in contact, they are often separated by small local faults.

3. Discussion

We describe persistent large-scale spatial properties of PFZR in the Mojave section of the SAF, based on geological mapping at several tens of sites, supplemented by more detailed mapping at selected sites. The results establish the PFZR as a general structural property of the SAF in the Mojave. In addition, we find that the distribution of exposed PFZR is asymmetric across the fault, with more than twice cumulative area of PFZR cropping out on the northeast side of the slip zone than on the southwest side.

The fault zone structure at any given location can be affected by numerous variables and local conditions. Dor et al. [29] discuss various factors that can produce uncertainties in the interpretation of geological mapping of the type done here. The discussed issues include the general problem of connecting dynamic rupture behavior at seismogenic depth with surface observations, influence of contrast in surface lithology on the symmetry properties of the damage pattern, possible effect of fault dip on asymmetry, complex history of the fault, the influence of geometrical and compositional complexities, migration of the active slipping zone, and more. A general way to reduce the above interpretation problems, adopted in our work, is to perform multi-signal multi-scale mapping of rock damage at multiple sites along the fault. The characteristics of the fault structure discussed in this study, combined with the work of Dor et al. [29], have multiple manifestations at different scales and different sites along the fault. This provides a basis for interpreting the data in terms of persistent rupture behavior and the large-scale structural properties of the fault at depth.

3.1. Geologic observations related to the possible depth of pulverization

There are several indications that pulverization of the mapped PFZR occurred at a relatively shallow depth.

First, the Punchbowl fault only 5 km southwest from the outcrops of pulverized rock bodies near the SAF, is interpreted to have been exhumed from about 2 to 4 km ([41], and references therein). In the lack of evidence for a differential vertical movement between the two faults, we can assume that this is the maximum exhumation depth for the SAF in this area as well. The SAF is located farther away from the locus of uplift in the San Gabriel Mountains when compared to the Punchbowl area. Displacement along the current trace of the SAF that is associated with our mapped PFZR occurred during or after the time of activity of the Punchbowl fault [42]. The observed terrains did not arrive from far away, where exhumation could be potentially larger, because the current strand of the SAF has only a few tens of km of displacement in this area (e.g. [36]). Therefore, the inferred maximum uplift of 2–4 km for the area of the Punchbowl fault on the mountain side of the SAF provides an upper bound for exhumation of the SAF itself.

Second, at various sites along the Mojave section of the SAF, there are several lines of direct evidence that the Mojave acted as a relatively stable block with only minor exhumation throughout the late Miocene to present: near Gorman, Miocene rocks of the Quail Lake Formation are exposed at elevations that are within a hundred meters or so of Pliocene rocks of the Hungry Valley Formation and younger late Quaternary formations, with depositional contact between them (i.e., those formations were not separated from each other by a vertical component of motion on dip slip faults). Similarly, middle Quaternary fans near Quail Lake are offset 15 km along the SAF and directly overlie the Miocene rocks. Elsewhere in the western Mojave, there are Miocene Lake deposits (e.g., Rainbow basin near Barstow) that show no significant uplift of the western Mojave since at least middle to late Miocene time, which is essentially the age of the modern San Andreas fault system [43]. The Victorville fan has been offset tens of kilometers laterally, but shows no uplift on the Mojave side in the Quaternary. Considering that some of the strands of the SAF along which we have identified PFZR are relatively young, we again argue that vertical motion during the timeframe of their activity must be small. These observations suggest that at least since the middle Miocene, deep exhumation of the fault zone is unlikely to have occurred, although uplift has resulted in the areas current elevation of more than 1 km. Other Plio-Quaternary formations along the SAF, such as the Anaverde and the Juniper Hills formations, were deposited in narrow basins resulting from small structural complexities (step-overs). It is not clear how much has been eroded but the consolidation is minor,

suggesting again only minor exhumation. In addition, middle to late Quaternary fans are preserved along the fault, indicating only minor incision in late Quaternary time.

Third, we have found that several sandstone and conglomerate units that were never deeply buried are damaged or perhaps even pulverized at levels that exceed the background damage level. This general observation puts the upper bound for damage generation and maybe pulverization to a possible depth of several hundreds of meters or less, although further characterization of the damage to sedimentary units along the SAF is needed in order to provide more accurate constraints for the pulverization process.

Forth, additional direct evidence that pulverization occurs at shallow depths is provided by studies [44,2] of pulverized quartzite in fresh rupture zones in South African gold mines. They analyzed rock-powder samples collected from the rupture zone of $M=3.7$ earthquake at depth of about 2 km (and near large internal free surfaces), and found that the grain size distribution and other properties of those samples is similar to those found in Tejon Pass. Pulverized quartzites are abundant in many fresh rupture zones in the mines [45], sometimes forming under minimal or even negligible confining stress.

Wilson [46] argued that pulverization at Tejon Pass could have potentially occurred at a depth of 4–9 km based on exhumation rates in the Transverse Ranges. Even if the estimated exhumation is correct, the observed pulverization could have occurred during or after the exhumation. Moreover, the exhumation estimates have large uncertainties. Ref. [42] has shown that crystalline rock domains like the Pelona/Orocopia schists and possibly source rocks to our mapped PFZR could have been exhumed from a great depth during the Clemens-Well, Fenner, San-Franciscuito phase of the SAF (20–17 and 13–12 Ma). Displacement and possibly some exhumation continued since 4–5 Ma in the same zone along the modern SAF. However, according to the reconstruction of Powell and Weldon [42], the modern trace of SAF, which has well defined and unique structural association with our mapped PFZR, may have re-occupied the same region that was active during that early phase of faulting, but not the exact same ancient trace that is delineated now by the (rotated and inactive) Clemens-Well, Fenner and San-Franciscuito faults. The tight structural association of the PFZR with the modern trace of the SAF implies that the pulverization we observe occurred during the modern activity of the SAF, after the main phase of the exhumation.

3.2. Correlation of mapping results with geophysical observations

A number of recent studies concluded that the low velocity seismic waveguides that produce trapped waves in the San Andreas, Landers, San Jacinto, and North Anatolian fault zones are generally limited to the upper ~3–5 km of the crust [47–50,34]. The seismic trapping structures have a width on the order of 100 m, similar to the lateral dimensions of the mapped body of PFZR, and are associated with strong reduction of seismic velocities (e.g., 30–50%) and strong attenuation (e.g., Q values of shear waves less than 10). The seismically imaged depth extent of the trapping structures correlates with the maximum inferred pulverization depth of Section 3.1, and the PFZR should have significant reduction of seismic velocities and significant increase of seismic attenuation due to the strong reduction of grain size and associated hydrological and chemical effects. In addition, recent imaging studies based on trapped and head waves indicate that the shallow damaged layers are asymmetric across the faults [34,35]. We thus suggest that the observed PFZR are the surface expression of the low velocity fault zone layers that act as seismic waveguides.

3.3. Relations of the mapping results to theoretical predictions

The observed coherent layer of PFZR with relatively shallow inferred pulverization depth and apparent asymmetric structure with respect to the principal slip zone requires a generation mechanism. This mechanism should depend on large-scale properties (rather than local site conditions), and should generate strong tensional stress field in the vicinity of the fault that can produce asymmetric long-term damage pattern in the upper few km of the crust. A curvature along the entire Mojave section of the SAF can produce asymmetric static stress field [51]. However, this is unlikely to produce the extreme grain reduction of the pulverized rocks (e.g., [2], this study) and the highly localized asymmetric pattern of gouge fabric found by Dor et al. [29]. As outlined in the introduction, mode II rupture along a material interface (e.g., [4,10–18]) provides a specific set of predictions that are compatible with our observations.

The parameter-space study of Ben-Zion and Shi [27] indicates that dynamic generation of rock damage during such ruptures, under realistic conditions of velocity contrast and material properties, is limited to the shallow portion of the crust. The events propagate preferentially in the direction of slip on the side with lower seismic velocities at seismogenic depth, while

damage is generated in the top few km on the side with faster seismic velocity, which is persistently on the tensional quadrant of the radiated seismic field for the preferred propagation direction.

The available seismic imaging studies in our area indicate [31–33] that the northeast side of the Mojave section of the SAF has higher seismic velocities than the southwest side. The mapped distribution of PFZR in Figs. 2–5 and the finer-scale observations of Dor et al. [29] show more damage on the higher velocity block. While the completeness of the mapping is affected by sites availability, the multiple observed manifestations of damage asymmetry across the SAF are compatible with the predictions for wrinkle-like ruptures along a material interface. The tensional stress produced by wrinkle-like ruptures may be aided by dynamic reduction of normal stress associated with the other mechanisms mentioned in the introduction, although this can not be tested at present in the absence of explicit predictions. However, none of the other mechanisms explains the observed correlation between the damage asymmetry and the velocity structure of the fault, and the existence of a preferred or more vigorous rupture direction which is necessary for the production of long-term asymmetric damage structure.

3.4. Comparison between the structures of the active SAF and exhumed faults of the SAF system

The general structure that we observe for the SAF in the Mojave includes a very narrow zone on the order of a few cm to a meter or so in which slip is localized, surrounded by a zone of strong damage on a scale of several tens of meters without significant shear parallel to the principal slip zone (in places we find several secondary or previously active slip zones). The deformation decreases gradually as a function of distance from the principal slip zone. This structure matches general characteristics of ancestral exhumed faults of the SAF system such as the Punchbowl and San Gabriel Faults ([52–54] and references therein).

In addition to the presented observations associated with the SAF, we have also recently observed a similar, tens of meters wide body of pulverized granite along the southern side of the Garlock fault on Tejon Ranch, with pulverization decreasing away from the active trace of the fault. PFZR can be seen in meters to tens of meters wide exposures southwest of the Little Rock Fault, west of Tierra Subida Rd. and north of the Anaverde Creek near Palmdale. Farther to the east exposures of similar scale appear between strands of the Little Rock fault and the SAF along Pallett Creek Rd. We also found PFZR in ~20 cm layer adjacent to the ultracataclasite of the

Punchbowl fault on the sandstone side where it is exposed near the top of the trail that climbs up from the Southfork Campground. Several outcrops of pulverized granodiorite, ranging in width from several tens of cm to several meters appear adjacent to the traces of the Southern and Northern Nadeau faults, where Mt. Emma Rd. crosses Little Rock Creek, and on Cheseboro Rd. about 1.2 km north of the junction with Mt. Emma Rd. (some outcrops of PFZR there may be related to the nearby trace of the Punchbowl fault). A layer of pulverized granodiorite on a similar scale bounds the northeast side of the fault core of an ancestral strand of the SAF, 300 m south of the active SAF east of where it crosses Little Rock Creek (near “Little Rock Creek Site” of Ref. [29]). The pulverization found in these faults is on a much smaller scale with respect to other fault zones and may reflect either different pulverization conditions or different pulverization process; it may also be related to the amount of displacement under ‘pulverization–generation conditions’.

On the other hand, we found a clear absence of pulverized rocks in the structure of the San Gabriel fault near the “Earthquake Fault site” of Ref. [55], and in several other sites along Big Tujunga Canyon Road and Angeles Crest Highway. In the San Gabriel fault and other cases of uplifted structures that have no PFZR, it is possible that the exhumation was to such a depth that the zone of PFZR has been eroded and is not preserved (if it indeed formed at depths shallower than the exhumation depth). Outcrops of granitic rocks adjacent to the active trace of the Elsinore fault near the junction of Hwy 79 and Hwy 76 appear to be almost intact. This is despite the presence of a near by large step-over that would have promote tensional stresses (Lake Henshaw). Whether the absence of PFZR from the exposed structure of a fault implies that no mechanism with sufficiently strong dynamic reduction of normal stress operated during its activity is a question we cannot answer at this point.

4. Summary

The observations made in this paper, combined with previous geologic and geophysical observations, suggest that PFZR along the Mojave section of the SAF consist of a ~100 m wide layer parallel to the principal slip zone of the fault. We infer that the observed pulverization occurred at shallow depths based on several lines of geologic observations and theory. Our results and the smaller scale observations of Dor et al. [29] suggest further that the layer of PFZR is not centered on the principal slip zone, but is shifted on average to the northeast side of the fault. This apparent damage asymmetry is compatible with a preferred or more vigorous northwest propagation direction of

earthquakes on the Mojave section of the SAF, which would have a damage-promoting tensional quadrant on the northeast side. This is also the side of the fault that has faster seismic velocities at seismogenic depth based on available imaging studies in the area [31–33]. A northwest preferred rupture direction is opposite the currently inferred rupture direction [56] for the 1857 Ft. Tejon earthquake. See a related discussion on this issue at Ref. [29].

The correlation between the apparent damage asymmetry and the side of the fault with faster seismic velocities at seismogenic depth, together with the inferred shallow pulverization depth, are consistent with theoretical predictions associated with wrinkle-like ruptures along a material interface [27]. In addition to explaining our observations, such a mode of rupture can be relevant to various important aspects of the mechanics and structure of large faults, including the general lack of melting products; suppression of branching, short rise-time of earthquake slip, effective constitutive laws, and expected seismic shaking hazard [4,15]. The SAF in the Mojave has several structural properties in common with ancestral exhumed faults of its system, although PFZR do not have an equal presence in all of those faults. The partial similarity between the structure of the SAF that is exposed at the surface and those exhumed structures lends support to our inferences on seismogenic processes along the SAF.

Acknowledgments

We thank Ze'ev Reches, Tom Dewers and Brent Wilson for discussions during joint field trips. The study was funded by the National Science Foundation (grant EAR-0409048) and the Southern California Earthquake Center (based on NSF cooperative agreement EAR-8920136 and United States Geological Survey cooperative agreement 14-08-0001-A0899). The manuscript benefited from constructive reviews by Matthew d'Alesio, an anonymous referee and Editor Rob van der Hilst.

Appendix A. Supplementary data

Supplementary data associated with this article can be found, in the online version, at [doi:10.1016/j.epsl.2006.03.034](https://doi.org/10.1016/j.epsl.2006.03.034).

References

- [1] J.N. Brune, Fault normal dynamic loading and unloading: an explanation for “nongouge” rock powder and lack of fault-parallel shear bands along the San Andreas fault, *EOS Trans. Am. Geophys. Union* 82 (47) (2001) (Abstract S22B-0655).
- [2] B. Wilson, T. Dewers, Z. Reches, J.N. Brune, Particle size and energetics of gouge from earthquake rupture zones, *Nature* 434 (2005) 749–752.
- [3] J.N. Brune, S. Brown, P.A. Johnson, Rupture mechanism and interface separation in foam rubber model of earthquakes: a possible solution to the heat flow paradox and the paradox of large overthrusts, *Tectonophysics* 218 (1993) 59–67.
- [4] Y. Ben-Zion, Dynamic rupture in recent models of earthquake faults, *J. Mech. Phys. Solids* 49 (2001) 2209–2244.
- [5] H.J. Melosh, Acoustic fluidization: a new geological process? *J. Geophys. Res.* 84 (1979) 7513–7520.
- [6] J. Lomnitz-Adler, Model for steady friction, *J. Geophys. Res.* 96 (1991) 6121–6131.
- [7] J.R. Rice, Fault stress states, pore pressure distributions, and the weakness of the San Andreas fault, *Fault Mechanics and Transport Properties of Rocks*, Academic, San Diego, Calif, 1992, pp. 475–503.
- [8] J. Byerlee, Model for episodic flow of high-pressure water in fault zones before earthquakes, *Geology* 21 (1993) 303–306.
- [9] S.A. Miller, A. Nur, D.L. Olgaard, Earthquakes as a coupled shear stress high pore pressure dynamical system, *Geophys. Res. Lett.* 23 (2) (1996) 197–200.
- [10] J. Weertman, Unstable slippage across a fault that separates elastic media of different elastic constants, *J. Geophys. Res.* 85 (1980) 1455–1461.
- [11] G.G. Adams, Self-excited oscillations of two elastic half-spaces sliding with constant coefficient of friction, *J. Appl. Mech.* 62 (1995) 867–872.
- [12] D.J. Andrews, Y. Ben-Zion, Wrinkle-like slip pulse on a fault between different materials, *J. Geophys. Res.* 102 (1997) 553–571.
- [13] K. Ranjith, J. Rice, Slip dynamics at an interface between dissimilar materials, *J. Mech. Phys. Solids* 49 (2001) 341–361.
- [14] Y. Ben-Zion, Y. Huang, Dynamic rupture on an interface between a compliant fault zone layer and a stiffer surrounding solid, *J. Geophys. Res.* 107 (2002), [doi:10.1029/2001JB000254](https://doi.org/10.1029/2001JB000254).
- [15] Y. Ben-Zion, D.J. Andrews, Properties and implications of dynamic rupture along a material interface, *Bull. Seismol. Soc. Am.* 88 (1998) 1085–1094.
- [16] A. Cochard, J.R. Rice, Fault rupture between dissimilar materials: ill posedness, regularization, and slip-pulse response, *J. Geophys. Res.* 101 (2000) 25321–25336.
- [17] Z. Shi, Y. Ben-Zion, Dynamic rupture on a bimaterial interface governed by slip-weakening friction, *Geophys. J. Int.* 164 (2006), [doi:10.1111/j.1365-246X.2006.02853.x](https://doi.org/10.1111/j.1365-246X.2006.02853.x).
- [18] G.B. Brietzke, Y. Ben-Zion, Examining tendencies of in-plane rupture to migrate to material interfaces, *Geophys. J. Int.*, in review (2006).
- [19] D.J. Andrews, R.A. Harris, The wrinkle-like slip pulse is not important in earthquake dynamics, *Geophys. Res. Lett.* 32 (2005) L23303, [doi:10.1029/2005GL02399](https://doi.org/10.1029/2005GL02399).
- [20] Y. Ben-Zion, A comment on “The wrinkle-like slip pulse is not important in earthquake dynamics” by Andrews and Harris, *Geophys. Res. Lett.* 33 (2006) L06310, [doi:10.1029/2005GL025372](https://doi.org/10.1029/2005GL025372).
- [21] R.H. Sibson, Brecciation processes in fault zones: Inferences from earthquake rupturing, *Pure Appl. Geophys.* 124 (1–2) (1986) 159–175, [doi:10.1007/BF00875724](https://doi.org/10.1007/BF00875724).
- [22] W.L. Power, T.E. Tullis, J.D. Weeks, Roughness and wear during brittle faulting, *J. Geophys. Res.* 93 (1988) 15268–15278.
- [23] T. Yamashita, Generation of microcracks by dynamic shear rupture and its effects on rupture growth and elastic wave radiation, *Geophys. J. Int.* 143 (2000) 395–406.

- [24] A.N. Poliakov, B.R. Dmowska, J.R. Rice, Dynamic shear rupture interactions with fault bends and off-axis secondary faulting, *J. Geophys. Res.* 107 (B11) (2002), doi:10.1029/2001JB000572.
- [25] L.A. Dalguer, K. Irikura, J.D. Riera, Simulation of tensile crack generation by three-dimensional dynamic shear rupture propagation during an earthquake, *J. Geophys. Res.* 108 (B3) (2003) 2144, doi:10.1029/2001JB001738.
- [26] D.J. Andrews, Rupture dynamics with energy loss outside the slip zone, *J. Geophys. Res.* 110 (2005) B01307, doi:10.1029/2004JB003191.
- [27] Y. Ben-Zion, Z. Shi, Dynamic rupture on a material interface with spontaneous generation of plastic strain in the bulk, *Earth Planet. Sci. Lett.* 236 (2005) 486–496, doi:10.1016/j.epsl.2005.03.025.
- [28] J.R. Rice, C.G. Sammis, R. Parsons, Off-fault secondary failure induced by a dynamic slip pulse, *Bull. Seismol. Soc. Am.* 95 (2005) 109–134.
- [29] O. Dor, T.K. Rockwell, Y. Ben-Zion, Geologic observations of damage asymmetry in the structure of the San Jacinto, San Andreas and Punchbowl faults in southern California: a possible indicator for preferred rupture propagation direction, *Pure Appl. Geophys.* 163 (2006), doi:10.1007/s00024-005-0023-9.
- [30] J.S. Scott, T.G. Masters, F.L. Vernon, 3-D velocity structure of the San Jacinto fault zone near Anza, California — I. P waves, *Geophys. J. Int.* 119 (1994) 611–626.
- [31] G.S. Fuis, R.W. Clayton, P.M. Davis, T. Ryberg, W.J. Lutter, D.A. Okaya, E. Hauksson, C. Prodehl, J.M. Murphy, M.L. Benthien, S.A. Baer, M.D. Kohler, K. Thygesen, G. Simila, G.R. Keller, Fault systems of the 1971 San Fernando and 1994 Northridge earthquakes, southern California: Relocated aftershocks and seismic images from LARSE II, *Geology* 31 (2003) 171–174.
- [32] W.J. Lutter, G.S. Fuis, T. Ryberg, D.A. Okaya, R.W. Clayton, P.M. Davis, C. Prodehl, J.M. Murphy, V.E. Langenheim, M.L. Benthien, N.J. Godfrey, N.I. Christensen, K. Thygesen, C.H. Thurber, G. Simila, G.R. Keller, Upper crustal structure from the Santa Monica Mountains to the Sierra Nevada, Southern California: tomographic results from the Los Angeles Regional Seismic Experiment, Phase II (LARSE), *Bull. Seismol. Soc. Am.* 94 (2004) 619–632.
- [33] N.M. Shapiro, M. Campillo, L. Stehly, M.H. Ritzwoller, High resolution surface wave tomography from ambient seismic noise, *Science* 307 (5715) (2005) 1615–1618, doi:10.1126/science.1108339.
- [34] M.A. Lewis, Z. Peng, Y. Ben-Zion, F. Vernon, Shallow seismic trapping structure in the San Jacinto fault zone, *Geophys. J. Int.* 162 (2005) 867–881, doi:10.1111/j.1365-246X.2005.02684.x.
- [35] M.A. Lewis, Y. Ben-Zion, J. McGuire, Imaging the deep structure of the Bear Valley section of the San Andreas Fault with joint analysis of fault-zone head and direct *P* wave arrivals, *Geophys. J. Int.*, in review (2006).
- [36] A.G. Barrows, J.E. Kahle, D.J. Beeby, Earthquake hazard and tectonic history of the San Andreas Fault Zone, Los Angeles County, California, Open File Report 85-10 LA, California Department of Conservation, Division of Mines and Geology, 1985.
- [37] Ross, D.C. Map showing recently active breaks along the San Andreas Fault between Tejon Pass and Cajon Pass, Southern California, USGS Miscellaneous Geologic Investigation, map I-553 (1969).
- [38] C.W. Jennings, R.G. Strand, T.H. Rogers (compilers), Geological map of California, Calif. Div. Mines and Geol., American Geological Institute (2001).
- [39] A. Schubnel, personal comm. (2005).
- [40] M.H. Anders, N. Christie-Blick, S. Wills, Rock deformation studies in the Mineral Mountains and Sevier Desert of west-central Utah: implications for upper crustal low-angle normal faulting, *Geol. Soc. Amer. Bull.* 113 (7) (2001) 895–907.
- [41] F.M. Chester, J.S. Chester, D.L. Kirschner, S.E. Schulz, J.P. Evans, Structure of large-displacement strike-slip fault zones in the brittle continental crust, in: Gary D. Karner, Brian Taylor, Neal W. Driscoll, David L. Kohlstedt (Eds.), *Rheology and Deformation in the Lithosphere at Continental Margins*, MARGINS Theoretical and Experimental Earth Science Series, vol. 1, Columbia University Press, New York, 2004, pp. 223–260.
- [42] R.E. Powell, R.J. Weldon, Evolution of the San Andreas Fault, *Annu. Rev. Earth Planet. Sci.* 20 (1992) 431–468.
- [43] M. Oskin, J. Stock, Marine incursion synchronous with plate-boundary localization in the Gulf of California, *Geology* 31 (2003) 23–26.
- [44] Z. Reches, T.A. Dewers, Gouge formation by dynamic pulverization during earthquakes, *Earth Planet. Sci. Lett.* 235 (1–2) (2005) 361–374.
- [45] O. Dor, Z. Reches, G. van Aswegen, Fault zones associated with the Matjhabeng earthquake, 1999, South Africa, Rockburst and Seismicity in Mines, RaSiM5 (Proceedings), South African Inst. of Mining and Metallurgy, 2001, pp. 109–112.
- [46] B. Wilson, Meso- and Micro-Structural Analysis of the San Andreas Fault at Tejon Pass, California, Unpublished Masters Thesis, University of Oklahoma, Norman, Oklahoma, 279 pp (2004).
- [47] Y. Ben-Zion, Z. Peng, D. Okaya, L. Seeber, J.G. Armbruster, N. Ozer, A.J. Michael, S. Baris, M. Aktar, A shallow fault zone structure illuminated by trapped waves in the Karadere–Duzce branch of the North Anatolian Fault, western Turkey, *Geophys. J. Int.* 152 (2003) 699–717.
- [48] V.A. Korneev, R.M. Nadeau, T.V. McEvilly, Seismological studies at Parkfield IX: fault-zone imaging using guided wave attenuation, *Bull. Seismol. Soc. Am.* 93 (2003) 1415–1426.
- [49] A. Michael, Y. Ben-Zion, Inverting fault zone trapped waves with a genetic algorithm, *EOS* 79 (1998) F584.
- [50] Z. Peng, Y. Ben-Zion, A.J. Michael, L. Zhu, Quantitative analysis of seismic trapped waves in the rupture zone of the 1992 Landers, California earthquake: evidence for a shallow trapping structure, *Geophys. J. Int.* 155 (2003) 1021–1041.
- [51] M.A. d'Alessio, written communication, 2006.
- [52] F.M. Chester, J.M. Logan, Implications for mechanical properties of brittle faults from observations of the Punchbowl fault zone, California, *Pure. Appl. Geophys.* 124 (1986) 79–106.
- [53] S.E. Schultz, J.P. Evans, Mesoscopic structure of the Punchbowl Fault, Southern California and the geologic and geophysical structure of active strike slip faults, *J. Struct. Geol.* (2000) 913–930.
- [54] Y. Ben-Zion, C.G. Sammis, Characterization of fault zones, *Pure Appl. Geophys.* 160 (2003) 677–715.
- [55] J.P. Evans, F.M. Chester, Fluid-rock interaction and weakening of faults of the San Andreas system: inferences from San Gabriel fault-rock geochemistry and microstructures, *J. Geophys. Res.* 100 (1995) 13007–13020.
- [56] D.C. Agnew, K.E. Sieh, A documentary study of the felt effects of the great California earthquake of 1857, *Bull. Seismol. Soc. Am.* 68 (6) (1978) 1717–1729.